Relativistic calculation of atomic N-shell ionization by protons

Mau Hsiung Chen
Lawrence Livermore National Laboratory, University of California, Livermore, California 94550

Bernd Crasemann
Department of Physics and Chemical Physics Institute, University of Oregon, Eugene, Oregon 97403

(Received 16 September 1985; revised manuscript received 19 February 1986)

Relativistic plane-wave Born-approximation calculations of cross sections for N-shell ionization of $_{83}$Bi and $_{92}$U by protons with incident energies from 0.02 to 5 MeV are reported. The calculations were carried out by using Dirac-Hartree-Slater wave functions. Binding-energy change and Coulomb deflection were taken into account. The relativistic cross sections are compared with values from nonrelativistic Hartree-Slater wave functions to study the effects of relativity. A test calculation with hydrogenic wave functions yields very different results. The only available measurements (for $_{74}$W), revised with a corrected $4d$ fluorescence yield, agree with present theoretical predictions for $E_1 \leq 0.1$ MeV but fall below theory by a factor of 6 above $E_1 = 0.4$ MeV. This glaring discrepancy invites further investigation.

I. INTRODUCTION

Existing calculations of cross sections for Coulomb ionization of atomic inner shells by proton impact have been carried out primarily in the plane-wave Born approximation (PWBA) with screened hydrogenic wave functions.[1-4] To go beyond the first Born approximation, the perturbed-stationary-state (PSS) approach including energy-loss, Coulomb-deflection, binding, polarization, and relativistic corrections (ECPSSR) was developed by Brandt and Lapicki.[5,6] To look into the effect of more realistic wave functions and of *ab initio* incorporation of relativity, we have performed a series of relativistic plane-wave Born-approximation (RPWBA) calculations of K-, L-, and M-shell ionization cross sections, using Dirac-Hartree-Slater (DHS) wave functions.[7-9] These DHS calculations have now been extended to N-subshell ionization cross sections. In this paper, we report on results for N_{1-7}-subshell ionization of $_{83}$Bi and $_{92}$U by protons and compare these new theoretical cross sections with nonrelativistic Hartree-Slater results in order to study the effects of relativity.

II. THEORETICAL METHOD

In the PWBA (Ref. 1), the differential cross section for ejection of an electron from a closed atomic S shell by heavy-charged-particle impact is

$$\left[\frac{d\sigma_S}{dE_f}\right]^{\mathrm{PWBA}} = \frac{4\pi}{\hbar^2} Z_1^2 e^4 \frac{M_1}{E_1}(2j_S+1)\int_{q_{\min}}^{q_{\max}} \frac{dq}{q^3}\,|F_{fi}(q)|^2 . \tag{1}$$

Here, E_f is the kinetic energy of the ejected electron, $\hbar q$ is the momentum transferred to that electron, and Z_1, M_1, and E_1 are the charge, mass, and initial kinetic energy of the projectile, respectively; j_S is the total angular momentum of the S-shell electron; and $F_{fi}(q)$ is the relativistic form factor. The exact limits of the momentum transfer[5,7] were used in the present calculations.

To take into account the effect caused by the presence of the slow charged projectile in the vicinity of the nucleus during the collision, the N-shell binding energy of the united atom (i.e., of the atom with atomic number Z_2+1 in the case of proton impact) was used in these calculations. This increase in binding energy tends to reduce the ionization cross section. The present procedure for correcting for the binding energy can be justified only when the projectile's velocity is much smaller than the orbital velocity of the N-shell electron. In the case treated here, however, the projectile velocity is actually comparable to the N-shell electron's orbital velocity, hence replacing the N-shell binding energy with the binding energy of the united atom will lead to an excessive binding correction. Furthermore, the polarization effect, which is not included, could reduce the binding energy.

The effect of the Coulomb repulsion between the projectile and the target nucleus on the N-subshell ionization was taken into account by applying a correction factor to the cross section calculated for a straight-line projectile path.[10,11] The differential cross sections including the Coulomb-deflection correction can be written as[10,11]

$$\left[\frac{d\sigma_N}{dE_f}\right]^{C} = \left[\frac{d\sigma_N}{dE_f}\right]^{\mathrm{PWBA}} \exp(-\pi d q_0) , \tag{2}$$

where

$$q_0 = (U_N + E_f)/v_1 . \tag{3}$$

Here, U_N is the binding energy of an N-shell electron, d is the half-distance between the collision partners at closest approach, and v_1 is the initial projectile speed.

A general computer program, written for calculating RPWBA ionization cross sections with DHS wave functions, was employed to evaluate the N_i-subshell Coulomb ionization cross sections. The atomic form factors were

calculated with neutral-atom DHS wave functions.[12,13] The form-factor integrals were computed by two successive fast Fourier transforms.[14] The detailed numerical procedure is described in Ref. 7.

Because the form factor is evaluated in a logarithmic mesh, the present approach is more suitable for inner-shell ionization calculations with compact bound-orbital wave functions and for low to intermediate collision energies. Therefore we limit our effort to heavy elements and intermediate incident-proton energies (see Sec. III).

Nonrelativistic Hartree-Slater (HS) wave functions were generated with the same DHS program by multiplying the speed of light by a factor of 1000 so as to simulate the nonrelativistic limit.[15,16] The same general program for evaluating relativistic ionization cross sections was then employed to calculate the HS PWBA cross sections for comparison with the relativistic results. Identical N_i-subshell binding energies from relativistic theory[13] were used in both DHS and HS calculations.

III. RESULTS AND DISCUSSION

In Table I we list the N_1-, N_2-, and N_3-subshell ionization cross sections calculated from the DHS model for $_{83}$Bi and $_{92}$U under proton impact with incident energies between 0.02 and 5 MeV. Results for the $N_{4,5}$ and $N_{6,7}$ subshells are listed in Table II. The theoretical values listed in Tables I and II are RPWBA cross sections as well as cross sections corrected for binding and Coulomb-deflection effects (RPWBA-BC). The PWBA cross sections from DHS and HS wave functions are compared in Figs. 1 and 2.

TABLE I. Relativistic plane-wave Born-approximation cross sections (RPWBA) (in barns), calculated from Dirac-Hartree-Slater wave functions for $N_{1,2,3}$-subshell ionization of Bi and U by protons of energy E_1 (in MeV). Numbers in square brackets indicate powers of 10; e.g., $1.05[3]=1.05\times10^3$.

	N_1		N_2		N_3	
E_1	RPWBA	RPWBA-BC	RPWBA	RPWBA-BC	RPWBA	RPWBA-BC
			$_{83}$Bi			
0.02	4.26[1]	9.46[−3]	1.21[2]	7.92[−2]	4.95[2]	1.04
0.04	2.51[2]	9.46	4.83[2]	3.20[1]	1.70[3]	1.72[2]
0.06	6.42[2]	1.05[2]	9.45[2]	1.95[2]	3.50[3]	8.82[2]
0.08	8.95[2]	2.77[2]	1.64[3]	5.23[2]	6.52[3]	2.37[3]
0.1	1.05[3]	3.92[2]	2.71[3]	9.83[2]	1.08[4]	4.51[3]
0.2	4.71[3]	2.47[3]	1.28[4]	7.62[3]	4.16[4]	2.70[4]
0.3	1.42[4]	9.16[3]	2.59[4]	1.81[4]	7.57[4]	5.59[4]
0.4	2.48[4]	1.80[4]	3.83[4]	2.91[4]	1.08[5]	8.48[4]
0.5	3.45[4]	2.68[4]	4.91[4]	3.92[4]	1.36[5]	1.11[5]
0.6	4.27[4]	3.47[4]	5.80[4]	4.79[4]	1.59[5]	1.34[5]
0.7	4.93[4]	4.13[4]	6.50[4]	5.51[4]	1.77[5]	1.53[5]
0.8	5.45[4]	4.67[4]	7.05[4]	6.09[4]	1.91[5]	1.68[5]
0.9	5.85[4]	5.11[4]	7.46[4]	6.55[4]	2.02[5]	1.80[5]
1.0	6.15[4]	5.46[4]	7.78[4]	6.92[4]	2.10[5]	1.89[5]
2.0	6.35[4]	6.07[4]	8.24[4]	7.84[4]	2.20[5]	2.10[5]
3.0	5.43[4]	5.29[4]	7.17[4]	6.95[4]	1.91[5]	1.85[5]
4.0	4.61[4]	4.52[4]	6.15[4]	6.01[4]	1.64[5]	1.60[5]
5.0	3.98[4]	3.91[4]	5.33[4]	5.23[4]	1.43[5]	1.40[5]
			$_{92}$U			
0.02	1.10[1]	7.5[−6]	1.84[1]	7.44[−5]	7.53[1]	3.03[−3]
0.04	2.64[1]	1.69[−1]	8.61[1]	9.58[−1]	3.61[2]	9.23
0.06	7.90[1]	4.06	1.92[2]	1.54[1]	7.34[2]	9.43[1]
0.08	1.88[2]	2.57[1]	3.12[2]	5.77[1]	1.18[3]	2.94[2]
0.1	3.06[2]	2.53[2]	4.38[2]	1.09[2]	1.77[3]	5.47[2]
0.2	6.49[2]	3.34[2]	1.82[3]	9.38[2]	7.60[3]	4.41[3]
0.3	1.78[3]	1.03[3]	4.54[3]	2.89[3]	1.72[4]	1.19[4]
0.4	4.14[3]	2.71[3]	8.09[3]	5.71[3]	2.84[4]	2.14[4]
0.5	7.20[3]	5.14[3]	1.20[4]	8.99[3]	3.99[4]	3.17[4]
0.6	1.05[4]	7.91[3]	1.57[4]	1.23[4]	5.11[4]	4.20[4]
0.7	1.37[4]	1.08[4]	1.93[4]	1.56[4]	6.14[4]	5.17[4]
0.8	1.67[4]	1.36[4]	2.24[4]	1.87[4]	7.06[4]	6.06[4]
0.9	1.94[4]	1.62[4]	2.53[4]	2.14[4]	7.86[4]	6.86[4]
1.0	2.18[4]	1.85[4]	2.76[4]	2.38[4]	8.54[4]	7.55[4]
2.0	3.23[4]	3.02[4]	3.64[4]	3.42[4]	1.14[5]	1.08[5]
3.0	3.17[4]	3.04[4]	3.49[4]	3.35[4]	1.09[5]	1.05[5]
4.0	2.87[4]	2.79[4]	3.15[4]	3.06[4]	9.86[4]	9.60[4]
5.0	2.57[4]	2.52[4]	2.80[4]	2.75[4]	8.83[4]	8.64[4]

TABLE II. Relativistic plane-wave Born-approximation cross sections (RPWBA) (in barns), calculated from Dirac-Hartree-Slater wave functions for $N_{4,5}$- and $N_{6,7}$-subshell ionization of Bi and U by protons of energy E_1 (in MeV).. Numbers in square brackets indicate powers of 10.

	N_4		N_5		N_6		N_7	
E_1	RPWBA	RPWBA-BC	RPWBA	RPWBA-BC	RPWBA	RPWBA-BC	RPWBA	RPWBA-BC
				$_{83}$Bi				
0.02	2.45[3]	2.94[1]	4.58[3]	6.64[1]	3.29[5]	5.05[4]	4.82[5]	7.60[4]
0.04	1.41[4]	2.34[3]	2.57[4]	4.69[3]	6.40[5]	2.71[5]	9.34[5]	4.03[5]
0.06	3.05[4]	1.06[4]	5.14[4]	1.90[4]	9.00[5]	5.02[5]	1.30[6]	7.33[5]
0.08	4.61[4]	2.20[4]	7.46[4]	3.71[4]	1.11[6]	7.03[5]	1.60[6]	1.02[6]
0.1	6.04[4]	3.17[4]	9.76[4]	5.20[4]	1.29[6]	8.07[5]	1.84[6]	1.16[6]
0.2	1.32[5]	9.24[4]	2.29[5]	1.60[5]	1.79[6]	1.36[6]	2.54[6]	1.93[6]
0.3	1.99[5]	1.53[5]	3.49[5]	2.70[5]	2.01[6]	1.63[6]	2.83[6]	2.31[6]
0.4	2.52[5]	2.04[5]	4.37[5]	3.57[5]	2.12[6]	1.78[6]	2.98[6]	2.51[6]
0.5	2.92[5]	2.45[5]	5.01[5]	4.24[5]	2.18[6]	1.87[6]	3.07[6]	2.64[6]
0.6	3.21[5]	2.76[5]	5.47[5]	4.73[5]	2.22[6]	1.93[6]	3.12[6]	2.72[6]
0.7	3.43[5]	3.00[5]	5.79[5]	5.10[5]	2.23[6]	1.97[6]	3.13[6]	2.77[6]
0.8	3.58[5]	3.17[5]	6.02[5]	5.37[5]	2.23[6]	1.99[6]	3.13[6]	2.79[6]
0.9	3.69[5]	3.31[5]	6.19[5]	5.58[5]	2.22[6]	2.00[6]	3.11[6]	2.80[6]
1.0	3.76[5]	3.41[5]	6.28[5]	5.71[5]	2.21[6]	2.00[6]	3.09[6]	2.80[6]
2.0	3.71[5]	3.53[5]	6.06[5]	5.78[5]	1.94[6]	1.82[6]	2.70[6]	2.54[6]
3.0	3.20[5]	3.09[5]	5.18[5]	5.01[5]	1.64[6]	1.56[6]	2.28[6]	2.17[6]
4.0	2.76[5]	2.68[5]	4.43[5]	4.32[5]	1.42[6]	1.36[6]	1.97[6]	1.89[6]
5.0	2.40[5]	2.34[5]	3.86[5]	3.77[5]	1.26[6]	1.21[6]	1.74[6]	1.67[6]
				$_{92}$U				
0.02	3.90[2]	2.01[−1]	7.08[2]	5.59[−1]	2.39[4]	4.27[2]	3.74[4]	7.68[2]
0.04	1.26[3]	7.28[1]	2.37[3]	1.58[2]	6.18[4]	1.35[4]	9.10[4]	2.07[4]
0.06	3.44[3]	6.44[2]	6.49[3]	1.33[3]	9.63[4]	3.90[4]	1.46[5]	6.01[4]
0.08	6.64[3]	2.10[3]	1.21[4]	4.11[3]	1.31[5]	6.86[4]	1.99[5]	1.06[5]
0.1	1.03[4]	4.06[3]	1.80[4]	7.46[3]	1.64[5]	8.84[4]	2.41[5]	1.32[5]
0.2	2.96[4]	1.92[4]	4.98[4]	3.27[4]	3.02[5]	2.20[5]	4.37[5]	3.22[5]
0.3	4.94[4]	3.66[4]	8.67[4]	6.46[4]	3.99[5]	3.19[5]	5.73[5]	4.61[5]
0.4	6.85[4]	5.42[4]	1.22[5]	9.72[4]	4.72[5]	3.94[5]	6.75[5]	5.66[5]
0.5	8.58[4]	7.05[4]	1.54[5]	1.27[5]	5.29[5]	4.53[5]	7.54[5]	6.48[5]
0.6	1.01[5]	8.53[4]	1.80[5]	1.53[5]	5.73[5]	4.99[5]	8.17[5]	7.14[5]
0.7	1.14[5]	9.83[4]	2.02[5]	1.76[5]	6.10[5]	5.38[5]	8.69[5]	7.69[5]
0.8	1.25[5]	1.10[5]	2.21[5]	1.95[5]	6.40[5]	5.70[5]	9.08[5]	8.12[5]
0.9	1.35[5]	1.20[5]	2.37[5]	2.11[5]	6.63[5]	5.96[5]	9.42[5]	8.49[5]
1.0	1.43[5]	1.28[5]	2.50[5]	2.25[5]	6.82[5]	6.17[5]	9.68[5]	8.78[5]
2.0	1.77[5]	1.67[5]	2.98[5]	2.83[5]	7.39[5]	6.96[5]	1.01[5]	9.53[5]
3.0	1.69[5]	1.63[5]	2.82[5]	2.72[5]	6.97[5]	6.65[5]	9.35[5]	8.94[5]
4.0	1.55[5]	1.50[5]	2.55[5]	2.48[5]	6.39[5]	6.15[5]	8.48[5]	8.18[5]
5.0	1.40[5]	1.36[5]	2.30[5]	2.24[5]	4.85[5]	5.65[5]	7.71[5]	7.46[5]

The present calculations were performed with a logarithmic integration mesh which becomes unsuitable in the asymptotic region. The maximum incident-proton energy was therefore chosen so that there are at least six mesh points per half cycle of the continuum-electron wave function, at a radial distance where the tail of the pertinent bound-electron wave function still contributes to the cross section. The reference bound state for applying this criterion was taken to be Bi $4f_{7/2}$, since this orbital has the most diffuse wave function of any N-shell orbital encountered in these calculations. The criterion then limits the incident-proton energy to ~ 5 MeV. Specifically, for 5-MeV proton impact, the contribution from the tail region ($r \geq 1.2$ a.u.) to the $4f_{7/2}$ ionization cross section of Bi is $\sim 1.5\%$. One can therefore conclude that use of the logarithmic integration mesh introduces negligible ($\leq 1\%$) error in the cross sections for all incident-proton energies included in the present calculations.

The binding correction reduces the N_i-subshell ionization cross sections by ~ 15–25% at $E_1 = 0.1$ MeV and by $\sim 8\%$ at $E_1 = 1$ MeV. Coulomb deflection leads to a reduction of N_i-subshell ionization cross sections by as much as a factor of 2 at $E_1 = 0.1$ MeV but by only 2.8% at $E_1 = 1$ MeV. For very low incident-proton energies, the Coulomb-deflection correction factor in Eq. (2) overestimates this effect.

Relativistic effects on the K-, L-, and M-subshell ionization cross sections have previously been found to be quite important.[7,8,16–18] For the N shell, we find substantial relativistic effects in the lowest two subshells. The N_1 ionization cross section is enhanced by as much as 50% for $_{83}$Bi and 80% for $_{92}$U if relativity is included. The N_2

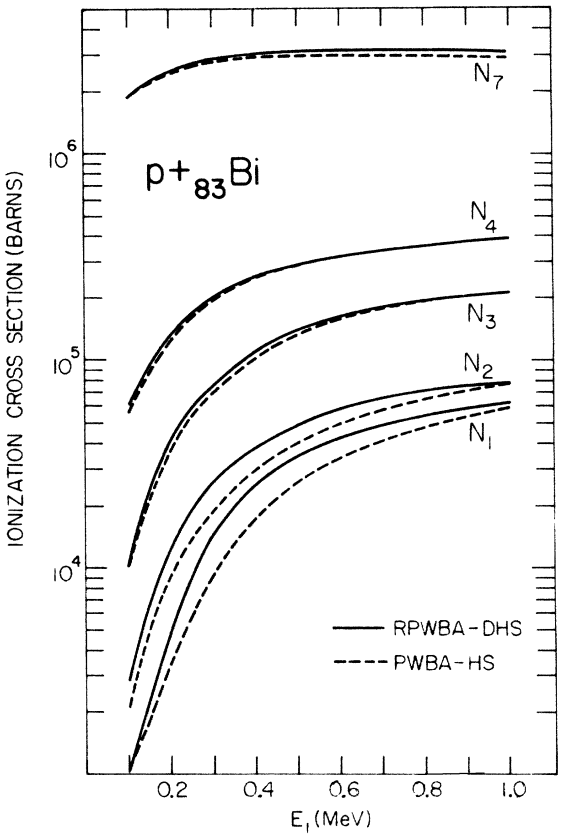

FIG. 1. Cross sections for N_i-subshell ionization of Bi by proton bombardment, as functions of incident-proton energy. Results of the present relativistic plane-wave Born-approximation calculations from Dirac-Hartree-Slater wave functions (solid curves) are compared with cross sections computed nonrelativistically from Hartree-Slater wave functions (dashed curves).

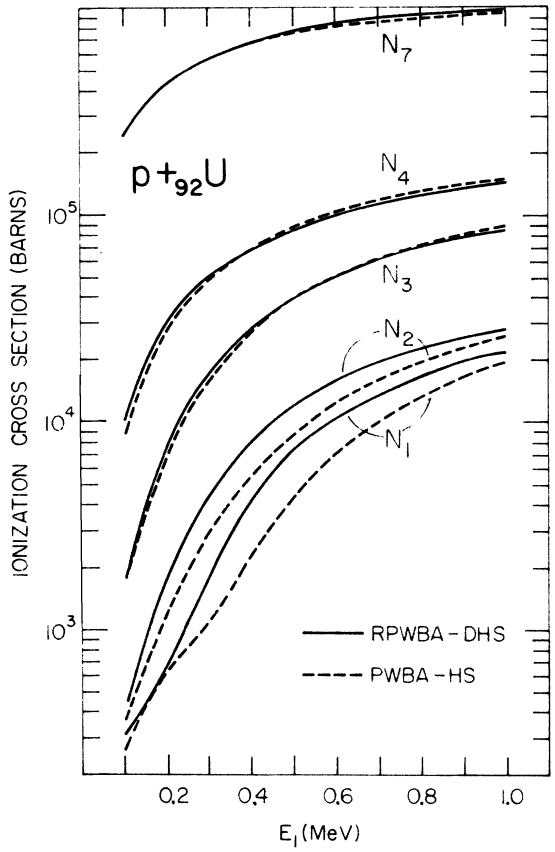

FIG. 2. Cross sections for N_i-subshell ionization of U by protons, as functions of incident-proton energy. Curves are identified in the caption of Fig. 1.

ionization cross section is enhanced by 35% for Bi and 45% for U. On the other hand, the ionization cross sections for the outer subshells N_3 through N_7 are affected by only a few percent when relativity is taken into account. The effect of relativity on the total N-shell ionization cross section can therefore be expected to be minimal, since the $N_{6,7}$-subshell cross sections are 1—2 orders of magnitude larger than the $N_{1,2}$ cross sections.

IV. COMPARISON WITH PREVIOUS WORK

Very little research on N-shell ionization is reported in the literature with which the present results could be compared. We find but one theoretical and one experimental paper. Sizov and Kabachnik[19] have calculated PWBA N-shell ionization cross sections for $_{54}$Xe with both hydrogenic and HS wave functions. Results from the two types of wave functions differ by as much as an order of magnitude.

The only published measurement of N-shell ionization by protons that we can find pertains to the $4d$ shell of $_{74}$W.[20] The authors compare their data with a calculation in the semiclassical approximation (SCA) that they performed with hydrogenic wave functions, and find good agreement.[20] On the other hand, tungsten $4d$ cross sections calculated through our present approach differ substantially from the experimental and theoretical results of Ref. 20, as shown in Fig. 3. Several points can be made regarding the discrepancies between the present theoretical results and those of Ref. 20.

Wave-function effect. The SCA ionization cross sections of Ref. 20 peak at a projectile energy for which the velocity of the projectile is one-half of the orbital velocity of the W $4d$ target electron. On the other hand, the $4d$-electron cross sections from the present calculation reach a maximum at an energy for which the projectile velocity is approximately equal to the orbital electron velocity. This latter result is consistent with the situation for K- and L-shell ionization,[9,21] for which the maximum in the cross sections is found to occur when the incident-proton velocity matches the velocity of the target electrons.

It appears likely that the unusually low peak energy of the calculated SCA cross sections in Ref. 20 might be due to errors that arise from the use of hydrogenic wave functions. We confirmed this surmise by calculating the W cross sections with our computer code, but programming it so as to use screened relativistic hydrogenic wave functions (SH). The result is very close to the SCA calculation of Ref. 20, as indicated by the dotted curve in Fig. 3. It is thus clear that the major discrepancy between the calculation of Ref. 20 and the present work can be traced to the use of hydrogenic wave functions in the former. This conclusion is consistent with the difference between the

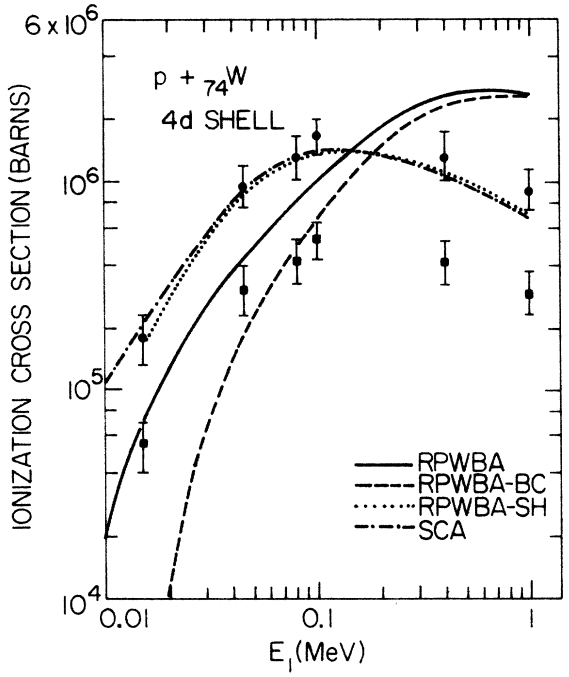

FIG. 3. Cross sections for $N_{4,5}$-subshell ionization of W by protons, as functions of incident-proton energy. Results of the present relativistic plane-wave Born-approximation calculations with Dirac-Hartree-Slater wave functions, without binding and Coulomb corrections (solid curve), and with binding and Coulomb corrections (dashed curve) are compared with cross sections computed in Ref. 20 with hydrogenic wave functions in the semiclassical approximation (dash-dotted curve). Present calculations with relativistic screened hydrogenic wave functions yield the dotted curve. The solid circles are experimental results from Ref. 20 based on the theoretical W $4d$ fluorescence yield from Ref. 22. The squares are these experimental cross sections revised by using the fluorescence yield calculated in the present work.

HS and hydrogenic results of Sizov and Kabachnik.[19]

Fluorescence yield. The $4d$-shell fluorescence yield of W (1.2×10^{-4}), used in Ref. 20 to convert x-ray yields to ionization cross sections, is taken from an independent-particle calculation.[22] It has, however, been shown that the calculated total $4d$ level widths for atoms with atomic numbers $70\leq Z\leq80$ are approximately twice as large as measured widths.[22,23] These discrepancies have been traced to the inadequacy of the independent-particle model for calculations of Coster-Kronig and super-Coster-Kronig transition rates.[24] A recent many-body calculation[25] of N-shell linewidths agrees quite well with experiment.

We have recalculated the N-shell fluorescence yield of W in the following manner. The total radiative rates for the $4d$ subshell were computed in the Dirac-Fock model[26,27] in both the Coulomb and length gauges. Results in the two gauges agree to within 15%. By combining the Dirac-Fock radiative rates in the length gauge and the total Auger rates from many-body theory,[25] we find the $4d$-subshell fluorescence yield of W to be 3.76×10^{-4}, which is larger by a factor of 3 than the fluorescence yield used in deriving the experimental data of Ref. 20.

The newly derived fluorescence yield can be used to revise the experimental cross sections of Ref. 20. These revised cross sections are included in Fig. 3. Our calculated DHS cross sections are seen to agree well with the revised experimental results for projectile energies $E\leq0.1$ MeV. For $E\geq0.4$ MeV, however, our theoretical cross sections exceed the measurements of Ref. 20 by a factor of 6. Additional experiments would be of interest.

ACKNOWLEDGMENTS

We thank William F. Ballhaus, Jr., Director of the NASA Ames Research Center (ARC), for permission to use the computational facilities of the Center, and thank the ARC Computational Chemistry and Aerothermodynamics Branch, particularly David M. Cooper, for their hospitality. We gratefully acknowledge the computational assistance of Mei Chi Chen. Robert Anholt kindly called our attention to Ref. 20. This work was performed in part under the auspices of the Department of Energy by the Lawrence Livermore National Laboratory under Contract No. W-7405-ENG-48. At the University of Oregon, this work was supported in part by the Air Force Office of Scientific Research under Contract No. F49620-85-C-0040.

[1]D. H. Madison and E. Merzbacher, in *Atomic Inner-Shell Processes*, edited by B. Crasemann (Academic, New York, 1975), Vol. 1, p. 1.
[2]O. Benka and A. Kropf, At. Data Nucl. Data Tables **22**, 219 (1978).
[3]D. E. Johnson, G. Basbas, and F. D. McDaniel, At. Data Nucl. Data Tables **24**, 1 (1979).
[4]G. S. Khandelwal, B. H. Choi, and E. Merzbacher, At. Data **1**, 103 (1969).
[5]W. Brandt and G. Lapicki, Phys. Rev. A **23**, 1717 (1981).
[6]W. Brandt and G. Lapicki, Phys. Rev. A **20**, 465 (1979).
[7]M. H. Chen, B. Crasemann, and H. Mark, Phys. Rev. A **26**, 1243 (1982).
[8]M. H. Chen, B. Crasemann, and H. Mark, Phys. Rev. A **27**, 2358 (1983).
[9]M. H. Chen and B. Crasemann, At. Data Nucl. Data Tables **33**, 217 (1985).
[10]J. Bang and J. M. Hansteen, K. Dan. Vidensk. Selsk. Mat.-Fys. Medd. **31**, No. 13 (1959).
[11]G. Basbas, W. Brandt, and R. Laubert, Phys. Rev. A **7**, 983 (1973).
[12]D. A. Liberman, D. T. Cromer, and J. T. Waber, Comput. Phys. Commun. **2**, 107 (1971).
[13]K.-N. Huang, M. Aoyagi, M. H. Chen, B. Crasemann, and H. Mark, At. Data Nucl. Data Tables **18**, 243 (1976).
[14]J. D. Talman, J. Comput. Phys. **29**, 35 (1978).
[15]I. P. Grant, B. J. McKenzie, P. H. Norrington, D. F. Mayers, and N. C. Pyper, Comput. Phys. Commun. **21**, 207 (1980).
[16]M. H. Chen, Phys. Rev. A **30**, 2082 (1984).
[17]T. Mukoyama and L. Sarkadi, Phys. Rev. A **23**, 375 (1981).

[18]T. Mukoyama and L. Sarkadi, Phys. Rev. A **25**, 1411 (1982).
[19]V. V. Sizov and N. M. Kabachnik, J. Phys. B **14**, 2013 (1981).
[20]H. Tittel and F. Bell, Z. Phys. A **287**, 143 (1978).
[21]D. D. Cohen and M. Harrigan, At. Data Nucl. Data Tables **33**, 255 (1985).
[22]E. J. McGuire, Phys. Rev. A **5**, 1043 (1972).
[23]J. C. Fuggle and S. F. Alvarado, Phys. Rev. A **22**, 1615 (1980).
[24]M. H. Chen, in *Atomic Inner-Shell Physics*, edited by B. Crasemann (Plenum, New York, 1985), p. 31.
[25]M. Ohno and G. Wendin, Phys. Rev. A **31**, 2319 (1985).
[26]I. P. Grant, B. J. McKenzie, P. H. Norrington, D. F. Mayers, and N. C. Pyper, Comput. Phys. Commun. **21**, 207 (1980).
[27]M. H. Chen, Phys. Rev. A **31**, 1449 (1985).